

# High-Speed and Highly Repeatable Polarization-State Analyzer for 40-Gb/s System Performance Monitoring

L.-S. Yan, *Member, IEEE*, X. Steve Yao, *Member, IEEE*, C. Yu, Y. Wang, L. Lin, Z. Chen, and A. E. Willner, *Fellow, IEEE*

**Abstract**—We demonstrate a fast (<1 ms), all solid-state, highly repeatable, and accurate polarization-state analyzer based on magneto-optic polarization switches. The module is further used for optical signal-to-noise-ratio performance monitoring in a  $14 \times 40$ -Gb/s wavelength-division-multiplexing system.

**Index Terms**—Monitoring, optical signal-to-noise ratio (OSNR), optics communications, polarization, polarization analyzer, polarization-state generation.

## I. INTRODUCTION

THE ABILITY to rapidly, repeatably, and inexpensively generate and analyze the polarization state of an optical signal is of paramount importance in many measurement applications, especially future optical performance monitoring of an active network [1], [2]. Some of the critical parameters of a data signal or device that can be measured with a polarization-state generator and analyzer are: birefringence, degree of polarization (DOP), state of polarization (SOP), polarization-dependent loss, polarization-mode dispersion (PMD), and optical signal-to-noise ratio (OSNR). In addition, the information obtained can be further applied to medical imaging such as polarization resolved coherent topology measurement [3], and fiber sensor systems [4].

The main components of polarization state generators (PSGs) and analyzers (PSAs) have conventionally been made of mechanical elements that tend to be large, slow, and expensive, as well as being prone to normal mechanical wear-and-tear. Ferroelectric liquid-crystal-based PSGs have also been previously reported [5], [6], but have issues including temperature stability and reliability. Various schemes for polarization analysis, including in-line, coupled, or terminated configurations, have been proposed [7]–[11] for different target applications (measurement or monitoring). Speed, accuracy, repeatability, and multichannel capability are the major concerns for such modules. A laudable goal would be a PSA composed completely of solid-state elements that is faster, smaller, less expensive, and more importantly, has higher repeatability, stability, and multichannel monitoring/analyzing capability.

In this letter, we report a novel PSA composed of a series of magneto-optic (MO) polarization switches and one quarter-wave plate for optical performance monitoring. The SOP/DOP of the signal can be obtained by measuring only four optical power levels at four polarization states, with a total response time of less than 1 ms. In addition to the fast response, superior repeatability, and stability, the PSA shows very high accuracy; thus, we are able to use it to demonstrate *in situ* optical OSNR performance monitoring of a data signal in a  $14 \times 40$ -Gb/s wavelength-division-multiplexing (WDM) system by measuring the instantaneous DOP value for each channel. The monitored results agree well with conventional OSNR measurements using an optical spectrum analyzer (OSA) within a 1.5-dB range.

## II. DEVICE CONFIGURATION

Magnetic-effect-based polarization control techniques have been studied in the last few years [12]–[14]. The principles and characteristics of a PSG using MO switches have already been shown in [12]. The six-state PSG in Fig. 1(a) consists of an optional input polarizer used for alignment, three pairs (six pieces total) of MO switches and a quarter-wave plate. This kind of structure can function as a PSA using only two pairs of MO switches [Fig. 1(b)], although we may still use the conjugate of Fig. 1(a) for easier calibration (this will be discussed elsewhere).

The MO switch rotates the SOP by a precise angle of around  $+22.5^\circ/-22.5^\circ$  when a positive/negative magnetic field above a saturation field level is applied. Therefore, when the two switches in a pair rotate in the same direction, the net rotation is  $+45^\circ$  or  $-45^\circ$ . On the other hand, if the two rotators rotate in opposite directions, the net SOP rotation is zero. Thus, up to six distinct polarization states ( $0^\circ, \pm 45^\circ, 90^\circ$ , left-hand-circular, and right-hand-circular) can be generated from different combinations of activation conditions with six polarization switches.

For this structure to function as a PSA, a photodiode is required to detect the output optical power following the MO switch assembly. Assuming lossless optical transmission, the Mueller matrix of the PSA can be derived as shown in (1), at the bottom of the next page, where  $\alpha, \beta, \gamma$ , and  $\delta$  are the relative rotation angles of each switches. If the Stokes vector  $S = (S_0, S_1, S_2, S_3)$  represents the input polarization state, then the output optical power ( $S_0^{\text{OUT}}$ ) is

$$S_0^{\text{OUT}} = \frac{1}{2} [S_0 + \cos 2(\alpha + \beta) \cos 2(\gamma + \delta) S_1 + \sin 2(\alpha + \beta) \cos 2(\gamma + \delta) S_2 + \sin 2(\gamma + \delta) S_3]. \quad (2)$$

Manuscript received August 31, 2005; revised December 12, 2005.

L.-S. Yan, X. S. Yao, L. Lin, and Z. Chen are with the General Photonics Corp. 5228, Chino, CA 91710 USA (e-mail: lryan@generalphotonics.com).

C. Yu, Y. Wang, and A. E. Willner are with the Department of Electrical Engineering-Systems, University of Southern California, Los Angeles, CA 90089 USA.

Digital Object Identifier 10.1109/LPT.2006.870130

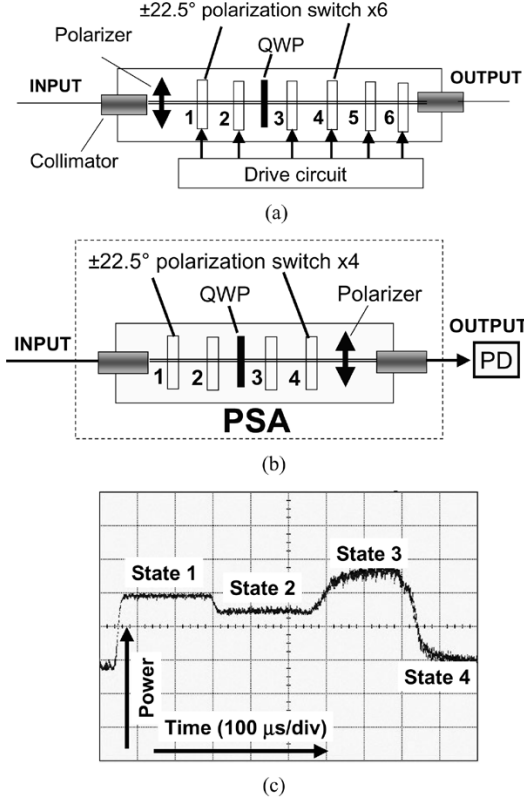


Fig. 1. (a) Configuration of a six-state PSG consisting of six MO polarization switches. (b) Configuration of PSA. (c) Typical response curve of the polarization state analyzer obtained by measuring optical power levels at four distinct polarization states (States 1 to 4).

Define  $\theta = \alpha + \beta$  and  $\varphi = \gamma + \delta$ , where  $\alpha = \beta = \gamma = \delta = \pm 22.5^\circ$ . Equation (2) can then be rewritten as

$$S_0^{\text{OUT}}(\theta, \varphi) = \frac{1}{2}[S_0 + S_1 \cos 2\theta \cos 2\varphi + S_2 \sin 2\theta \cos 2\varphi + S_3 \sin 2\varphi]. \quad (3)$$

Since the possible combinations of double-stage rotation angles  $(\theta, \varphi)$  can only be selected from combinations of  $45^\circ$ ,  $0^\circ$  and  $-45^\circ$ , by measuring the optical power at the four resultant polarization states, the SOP of the input signal can be obtained using the following equations:

$$S_0 = S_0^{\text{OUT}}(45^\circ, 0^\circ) + S_0^{\text{OUT}}(-45^\circ, 0^\circ) \quad (4)$$

$$S_1 = 2S_0^{\text{OUT}}(0^\circ, 0^\circ) - S_0^{\text{OUT}}(45^\circ, 0^\circ) - S_0^{\text{OUT}}(-45^\circ, 0^\circ), \quad (5)$$

$$S_2 = S_0^{\text{OUT}}(45^\circ, 0^\circ) - S_0^{\text{OUT}}(-45^\circ, 0^\circ) \quad (6)$$

$$S_3 = 2S_0^{\text{OUT}}(0^\circ, 45^\circ) - S_0^{\text{OUT}}(45^\circ, 0^\circ) - S_0^{\text{OUT}}(-45^\circ, 0^\circ). \quad (7)$$

TABLE I  
MEASUREMENT ACCURACY AND REPEATABILITY OF PSA FOR DIFFERENT POLARIZATION STATES OF LIGHT AT 1550 nm

Polarization State		$s_1$	$s_2$	$s_3$	DOP
Linearly Polarized (LP)	$\bar{s}_i$	-0.05849	0.998288	-0.00046	0.9999
	$\sigma_{s_i}$	0.00045	$2.6 \times 10^{-5}$	0.00043	0.00032
	$s_{i \max} - s_{i \min}$	0.00230	0.00013	0.00207	0.00200
Circularly Polarized (RCP)	$\bar{s}_i$	0.083803	0.008809	0.996443	0.9996
	$\sigma_{s_i}$	0.00025	0.000211	$2.1 \times 10^{-5}$	0.000257
	$s_{i \max} - s_{i \min}$	0.001065	0.001055	$9.22 \times 10^{-5}$	0.001035
Elliptically Polarized (EP)	$\bar{s}_i$	-0.59354	0.01514	-0.80466	0.998461
	$\sigma_{s_i}$	0.000548	0.000388	0.000404	0.000697
	$s_{i \max} - s_{i \min}$	0.003212	0.002366	0.002369	0.003134

where  $S_0^{\text{OUT}}(\theta, \varphi)$  is the detected optical power at different polarization switch conditions. Only four combinations of control logic are needed to obtain the input SOP information. Due to the short response time of MO switches ( $\sim 200 \mu\text{s}$ ), the total response time of the PSA is less than 1 ms, as shown in Fig. 1(c). (The electrical noise in the figure is partially due to the high bandwidth of the photodetector and the synchronization of trigger signals, which can easily be removed in real measurements.) Furthermore, we evaluated the accuracy and repeatability of the PSA using several fixed polarization states at 1550 nm. Table I shows the measurement results of the PSA after calibration, where  $\bar{s}_i$  is the average value of over 100 measurements,  $\sigma_{s_i}$  is the standard deviation, and  $s_{i \max} - s_{i \min}$  is the difference between maximum and minimum measurement values. The results show that the standard deviations of the SOP and DOP are less than 0.1% and 0.07%, respectively, while the maximum deviations for both are  $\sim 0.3\%$ , with a resolution of  $\sim 0.001$ ; such high accuracy and repeatability are highly desirable features in both measurement and monitoring, and much higher than regular polarimeters (typically  $\pm 2\%$  DOP accuracy for low-cost polarimeters, while  $< 1\%$  for high accuracy analyzers).

### III. OSNR PERFORMANCE MONITORING USING PSA

As a demonstration of a systems application of our PSA, we use the PSA as a performance monitor, to measure OSNR using the obtained SOP/DOP information. OSNR monitoring using the DOP of the signal is a well-known technique based on the fact that the optical signal is polarized while the optical noise is not. The relationship between DOP and OSNR is as simple as  $\text{OSNR} = \text{DOP}/(1 - \text{DOP})$ . To verify the functionality of our PSA, we first use a simple setup combining an optical signal from a tunable laser with a broad-band amplified spontaneous emission (ASE) source [Fig. 2(a)]. Then, an optical filter (OF) is placed between the PSA and the photodiode to filter out the signal. The obtained SOPs [denoted by the three Stokes parameters shown in Fig. 2(b)] at different signal power levels show the

$$M(T) = \frac{1}{2} \begin{pmatrix} 1 & \cos 2(\alpha + \beta) \cos 2(\gamma + \delta) & \sin 2(\alpha + \beta) \cos 2(\gamma + \delta) & \sin 2(\gamma + \delta) \\ 1 & \cos 2(\alpha + \beta) \cos 2(\gamma + \delta) & \sin 2(\alpha + \beta) \cos 2(\gamma + \delta) & \sin 2(\gamma + \delta) \\ 0 & 0 & 0 & 0 \\ 0 & 0 & 0 & 0 \end{pmatrix} \quad (1)$$

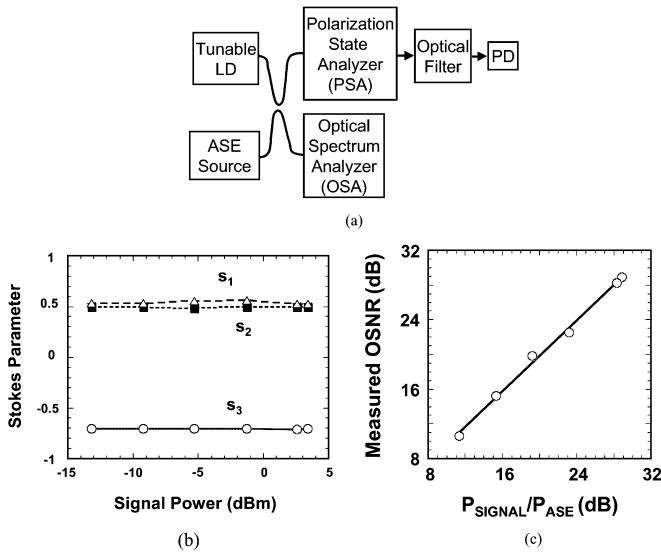


Fig. 2. OSNR monitoring (a) setup. (b) Measured SOP stability as a function of signal power. (c) Comparison of OSNR measured using PSA (vertical axis) with OSNR measured with conventional OSA (horizontal axis).

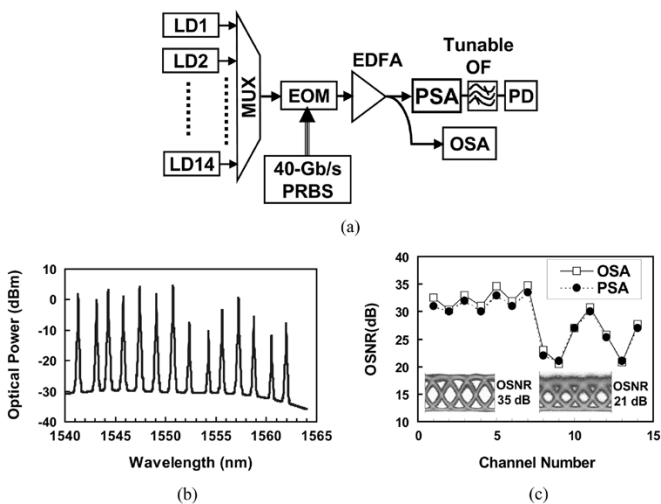


Fig. 3. System demonstration of performance monitoring (a) experimental setup of  $14 \times 40$ -Gb/s transmission system. (b) Optical spectrum measured after EDFA. (c) Comparison of monitored OSNR of each channel using PSA and commercial OSA.

repeatability and stability of the PSA, and the OSNR calculated from the DOP measured using the PSA is comparable to that measured by a commercial OSA, as shown in Fig. 2(c). Due to the power limits of our tunable laser and ASE source, the monitor range is only demonstrated from 10 to 30 dB. In this range, the results agree well with those measured by an OSA (0.1-nm bandwidth).

Furthermore, a system demonstration of OSNR monitoring is performed in a  $14 \times 40$ -Gb/s WDM transmission link with the setup shown in Fig. 3(a). All 14 channels are set at different power levels; thus, after the signal passes through an erbium-doped fiber amplifier (EDFA), the OSNR of each channel will be different. The optical spectrum of all of the channels

after the EDFA is shown in Fig. 3(b). By scanning the tunable OF, we can obtain the OSNR for each channel and compare it to OSA measurements. The results of this comparison are shown in Fig. 3(c), with two typical eye diagrams inserted (corresponding to OSNRs of 35 and 21 dB, respectively). The OSNR monitoring results using the PSA are close to the measurements using the OSA (at a relative bandwidth of  $\sim 0.4$  nm), with a maximum deviation of 1.5 dB (OSNR > 30 dB). The error is mainly due to high calculation sensitivity at high OSNR (>30 dB) using DOP. Note that DOP-based OSNR monitoring will be affected by the PMD of the link, which we do not consider here. Although an OF is used in this setup, a more practical solution is to place a demultiplexer (DEMUX) after the PSA. Each WDM channel will then have a separate photodetector, instead of using only one photodetector inside the PSA; thus, all of the channels can share one PSA module and perform the monitoring function simultaneously. Integrated DEMUX and photodetector assemblies are commercially available and can make the configuration compact and cost-effective.

REFERENCES

- [1] M. Petersson, H. Sunnerud, M. Karlsson, and B. E. Olsson, "Performance monitoring in optical networks using Stokes parameters," *IEEE Photon. Technol. Lett.*, vol. 16, no. 2, pp. 686–688, Feb. 2004.
- [2] D. C. Kilper, S. Chandrasekhar, L. Buhl, A. Agarwal, and D. Maywar, "Spectral monitoring of OSNR in high-speed networks," in *Proc. Eur. Conf. Optical Communication (ECOC 2002)*, Copenhagen, Denmark, Sep. 2002, Paper 7.4.4.
- [3] B. H. Park, M. C. Pierce, B. Cense, and J. F. de Boer, "Jones matrix analysis for a polarization-sensitive optical coherence tomography system using fiber-optic components," *Opt. Lett.*, vol. 29, no. 21, pp. 2512–2514, 2004.
- [4] L. R. Jaroszewicz and P. Marc, "Inline fiber-optic polarization analyzers for sensor application," *IEEE Sensors J.*, vol. 3, no. 1, pp. 71–79, Feb. 2003.
- [5] R. M. Craig, S. L. Gilbert, and P. D. Hale, "High-resolution, nonmechanical approach to polarization-dependent transmission measurements," *J. Lightw. Technol.*, vol. 16, no. 7, pp. 1285–1294, Jul. 1998.
- [6] W. Xiang and A. M. Weiner, "Fast multi-wavelength polarimeter for polarization mode dispersion compensation systems," in *Dig. LEOS Summer Topical Meetings*, 2003, pp. WB2.4/67–WB2.4/68.
- [7] P. Westbrook, L. Moller, S. Chandrasekhar, R. Dutta, and S. Wielandy, "Wavelength sensitive polarimeter for multichannel polarization and PMD monitoring," in *Proc. OFC 2002*, Anaheim, CA, 2002, Paper WK5.
- [8] L. Moller, P. Westbrook, S. Chandrasekhar, R. Dutta, and S. Wielandy, "SOP and PMD monitoring with WDM polarimeter," *Electron. Lett.*, vol. 38, no. 12, pp. 583–585, Jun. 2002.
- [9] R. Llorente, R. Clavero, and J. Marti, "PMD monitoring by spectral SOP rotation using a real-time optical fourier transformer," in *Proc. OFC 2005*, Anaheim, CA, 2005, Paper OME26.
- [10] B. Acharya, C. Madsen, K. Baldwin, R. Macharrie, J. Rogers, L. Moeller, C. Huang, and R. Pindak, "In-line liquid crystal microcell polarimeters and waveplates for high speed polarization analysis and control," in *Proc. OFC 2003*, Atlanta, GA, 2003, Paper WC2.
- [11] K. Hirabayashi and C. Amano, "A compact in-line polarimeter using a Faraday rotator," *IEEE Photon. Technol. Lett.*, vol. 15, no. 12, pp. 1740–1742, Dec. 2003.
- [12] X.-S. Yao, L.-S. Yan, and Y. Shi, "A Highly repeatable all solid-state polarization state generator," *Opt. Lett.*, vol. 30, no. 11, pp. 1324–1326, 2005.
- [13] T. Saito and S. Kinugawa, "Magnetic field rotating-type faraday polarization controller," *IEEE Photon. Technol. Lett.*, vol. 15, no. 10, pp. 1404–1406, Oct. 2003.
- [14] K. Ikeda, "Arbitrary polarization controller with variable Faraday rotator," in *National Fiber Optic Engineers Conf. (NFOEC 2002)*, Dallas, TX, Sep. 2002, p. 1965.